MALAYSIAN JOURNAL OF SCIENCE
MJS
ISSN 1394-3065

Regular Issue

Malaysian Journal of Science 44 (3): 27-49 (September 2025) https://mjs.um.edu.my

Effect of Shape on Strength and Durability of Crushed and Uncrushed Quartzite Aggregates from Central Nepal Himalaya

Dinesh Raj Sharma [1a] and Naresh Kazi Tamrakar[2a]*

Abstract: This study examines the influence of shape on the strength and durability of angular (crushed) and rounded (uncrushed) quartzite aggregates sourced from the Central Nepal Himalaya. Crushed quartzite samples, characterized by angular morphologies, exhibit enhanced interlocking and greater variability in mechanical properties such as Point Load Strength Index (PLSI), Aggregate Impact Value (AIV), and Aggregate Crushing Value (ACV), due to their rough textures. In contrast, rounded (uncrushed) quartzite from alluvial gravels, with subrounded particles, demonstrates more consistent strength and durability, as evidenced by narrower ranges in PLSI, AIV, and ACV. Durability tests, including Slake Durability Index (SDI), Los Angeles Abrasion Value (LAAV), and Sulfate Soundness Value (SSV), indicate that angular aggregates provide superior abrasion resistance, whereas subrounded aggregates display more uniform resistance to sulfate-induced weathering. These findings offer valuable insights for selecting quartzite aggregates based on shape to optimize performance in construction applications.

Keywords: *Quartzite, aggregates, aggregate shape, strength and durability.*

1. Introduction

Aggregates are essential components in construction. They are classified into two primary types: crushed and uncrushed. Crushed aggregates are generated by mechanically fragmenting larger rocks, boulders, or stones into smaller, angular particles (Neville & Brooks, 2015). Characteristics of crushed aggregates include an angular shape, rough and irregular surfaces with sharp edges and corners. The interlocking shape of crushed aggregates enhances the strength and durability of concrete used in railroad ballast. These aggregates also provide effective drainage and support for railroad tracks. In road base construction, the angular shape contributes to a stable and compacted foundation. Mixed crushed rocks can be incorporated into asphalt mixtures to improve strength and stability (Aïtcin, 2014). Uncrushed aggregates, also referred to as natural or rounded aggregates, are sourced directly from natural environments such as riverbeds, gravel pits, or quarries without mechanical crushing (Hachani et al., 2017). These aggregates typically exhibit rounded or sub-angular shapes with smoother surfaces and edges than crushed aggregates.

Angular aggregates offer superior interlocking and resistance to displacement compared to rounded or smooth aggregates. This interlocking effect often results in increased strength (Neville, 2011). Angular aggregates enhance bonding, thereby improving strength and durability (Mehta & Monteiro, 2006). Conversely, flat and elongated particles may create weak points that reduce the overall strength and durability (ACI 221R-96, 1996). Well-graded aggregates comprising a range of sizes can optimize packing density, potentially increasing strength (ACI 211.1, 1991). Smaller aggregates fill gaps between larger particles, reducing voids and improving the overall strength and durability of the aggregate matrix (Neville, 2011). The morphology of rock particles significantly affects their strength and durability, both critical for assessing suitability in diverse engineering applications. Strength parameters such as the Point Load Strength Index (PLSI), Aggregate Impact Value (AIV), and Aggregate Crushing Value (ACV) assess rocks' resistance to crushing and impact. Durability, defined as the long-term resistance to weathering and abrasion, is evaluated using tests like the Slake Durability Index (SDI), Los Angeles Abrasion Value (LAAV), and Sulphate Soundness Value (SSV) (Erguler & Ulusay, 2009; Gautam & Shakoor, 2013; Gökceoğlu et al., 2000). Rock shape influences these properties, with more angular rocks typically displaying superior strength and durability due to enhanced interlocking and diminished particle movement.

In the Lesser Himalaya and Sub-Himalaya regions, numerous studies have investigated the strength and durability attributes of rocks for engineering applications as aggregates. These studies reveal a strong correlation between texture and rock strength in quartzites from the Himalaya (Dhakal et al., 2006; Khanal & Tamrakar, 2009; Maharjan & Tamrakar, 2007; Tamrakar et al., 2003; Gupta & Sharma, 2012; Ahameda et al., 2017). Similarly, research has identified quartzite and its aggregates as among the

Authors information:
[a]Tribhuvan University, Central Department of Geology, Tribhuvan University, Kirtipur, Kathmandu, NEPAL. E-mail: dineshrajsharma@hotmail.com[1];
naresh.tamrakar@cdgl.tu.edu.np[2]
*Corresponding Author: naresh.tamrakar@cdgl.tu.edu.np2

Received: July, 2024
Accepted: June, 2025
Published: September, 2025

DOI:https//doi.org/10.22452/mjs.vol44no3.4
Malaysian Journal of Science 44(3): 27-49 (September 2025)

strongest and most durable rock types (Bista & Tamrakar, 2015; Maharjan & Tamrakar, 2007). The shape of aggregate particles influences strength and durability; however, investigations on this aspect remain scarce in the Himalayan region. Accordingly, four quartzite-rich litho-units from the Central Nepal Lesser Himalaya and one alluvial fan deposit from the Sub-Himalayan region (Figure 1) have been selected for sampling quartzite rocks and sediments, respectively. The principal objectives of the present study are to elucidate the effects of quartzite aggregate shapes on their strength and durability characteristics independently.

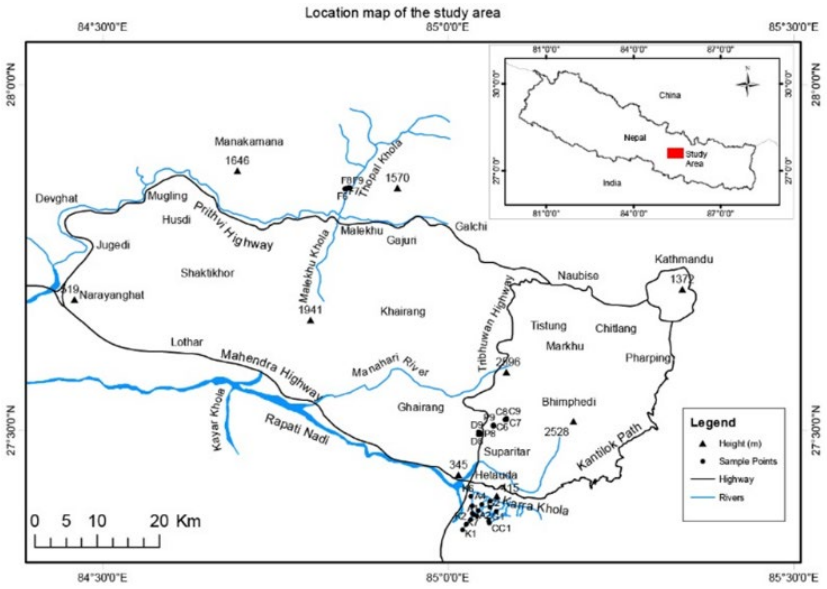

Figure 1. Location map of the study area

2. Geological Setting of Study Area

In the Nepal Himalaya, particularly in the Central Nepal Lesser Himalaya (Figure 2; Table 1), there are abundant deposits of quartzite beds within various lithostratigraphic units, namely Fagfog Quartzite, Dunga Quartzite, Pandrang Quartzite, and Chisapani Quartzite (Stöcklin 1980). In contrast, quartzite gravels are extensively distributed in the Sub-Himalaya (Figure 2; Table 1). The principal geological and tectonic units in the Lesser Himalaya are the Kathmandu Complex and the Nawakot Complex, representing the allochthonous and autochthonous series of the Mahabharat Synclinorium, respectively (Stöcklin & Bhattarai, 1977). The Nawakot Complex can be further subdivided into the Upper Nawakot Group and the Lower Nawakot Group, while the Kathmandu Complex is divided into the Phulchauki Group and Bhimphedi Group (Stöcklin & Bhattarai, 1977) (Table 1).

The research area for crushed quartzite aggregate is located in the Central Nepal Lesser Himalaya (Figure 2), where the Fagfog Quartzite and the Dunga Quartzite belong to the Lower Nawakot Group and the Upper Nawakot Group, respectively. The Dunga Quartzite is a member of the Robang Formation (Table 1). The Pandrang Quartzite belongs to the Kalitar Formation. Both the Kalitar Formation and the Chisapani Quartzite belong to the Upper Nawakot Group. All these quartzite lithostratigraphic units date to the Precambrian (Table 1).

The research area for uncrushed quartzite aggregate is situated in the Hetauda Dun in the Central Nepal Sub-Himalaya or Siwaliks (Figure 1 and 2). The Dun valley consists of Post-Siwalik sediments (Kimura, 1994; Schelling et al., 1991), dominantly composed of gravels and subordinately of sand, which were reworked from the Siwalik Group of rocks in the hilly range and deposited in river terraces as well as in alluvial fans. These Post-Siwalik sediments overlie the Siwalik Group of siliciclastic rocks, which are sparsely exposed along stream beds. The Siwalik Group is divided into three lithostratigraphic units: the Lower, Middle, and Upper Siwaliks (Hagen, 1969; Itihara et al., 1972; West & Munthe, 1981), which coarsen progressively upward, and belong to the Middle Miocene to the Early Pleistocene (Gautam & Rosler, 1999).

DOI:https//doi.org/10.22452/mjs.vol44no3.4
Malaysian Journal of Science 44(3): 27-49 (September 2025)

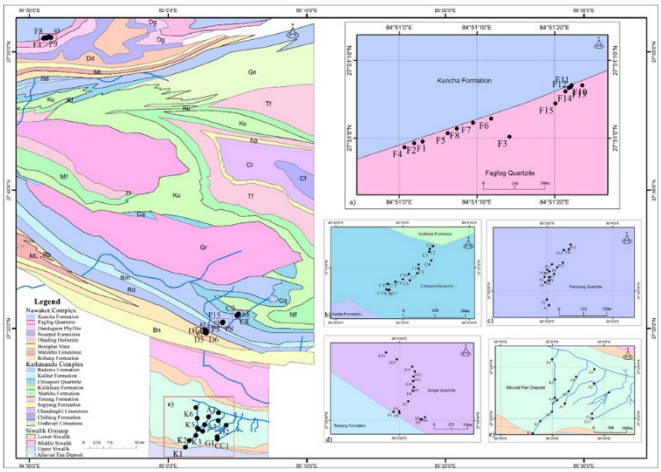

Figure 2. Geological map of study area and location of sample sites

Table 1. The Himalayan units in Central Nepal (Stöcklin and Bhattarai 1977)

Unit		Formation	Main Lithology	Apparent Thickness (m)	Age
Post-Siwalik Deposit			Boulder, cobble pebble Gravel, Sand	<50 m?	Mid to Late Pleistocene
Siwalik Group		Sandstone, mudstone, conglomerate	Several Kilometers	6000	Neogene
————————Main Boundary Thrust (MBT) ————————					
	Phulchauki Group	Godavari Limestone	Limestone, dolomite	300	Devonian
		Chitlang Formation	Slate	1,000	Silurian
		Chandagiri Limestone	Limestone	2,000	Cambro – Ordovician
		Sopyang Formation	Calc-phyllite, slate	200	Cambrian
		Tistung Formation	Metasandstone, phyllite	3,000	Late Precambrian
	————————Transitional Contact ————————				
Kathmandu Complex	Bhimphedi Group	Markhu Formation	Marble, schist	1,000	Late Precambrian
		Kulikhani Formation	Quartzite, schist	2,000	
		*Chisapani Quartzite	White Quartzite	400	
		*Kalitar Formation	Schist, quartzite (Pandrang Quartzite Member)	2,000	Precambrian
		Bhainsedobhan Marble	Marble	800	
		Raduwa Formation	Garnetiferous schist	1,000	
————————-Mahabharat Thrust (MT) ————————					
Nawakot Complex	Upper Nawakot Group	*Robang Formation	Phyllite, quartzite (Dunga Quartzite Member)	200 – 1,000	Paleozoic
		Malekhu Limestone	Limestone, Dolomite	800	
		Benighat Slate	Slate, argillaceous dolomite	500 – 3,000	
	———————— Unconformity (?)————————				
	Nawakot Lower Group	Dhading Dolomite	Stromatolitic dolomite	500 – 1,000	Late Precambrian
		Nourpul Formation	Phyllite, quartzite, dolomite	800	
		Dandagaon Phyllite	Phyllite	1,000	
		*Fagfog Quartzite	White quartzite	400	
		Kuncha Formation	Phyllite, quartzite, Conglomerate, gritstone	5,000	

*Formations considered in this study

DOI:https//doi.org/10.22452/mjs.vol44no3.4
Malaysian Journal of Science 44(3): 27-49 (September 2025)

3. Methodology

The shape of aggregates influences the strength and durability of construction materials; therefore, we conducted a comprehensive study comparing the strength and durability of crushed and uncrushed aggregates. Crushed aggregates were sourced from the bedrocks of four geological formations, namely the Fagfog Quartzite, Dunga Quartzite, Pandrang Quartzite, and Chisapani Quartzite of the Lesser Himalaya, while uncrushed aggregates were collected from alluvial fan gravels of the Siwalik region (Table 1; Figure 2). Fifteen samples from each stratigraphic unit were selectively collected to represent the studied units. Uncrushed samples were sieved into different size fractions and thoroughly cleaned to remove impurities before testing.

All crushed samples were angular to very angular, whereas uncrushed samples were all rounded. Angular and rounded aggregate particles were tested separately for strength (Point Load Strength Index (PLSI), Aggregate Impact Value (AIV), and Aggregate Crushing Value (ACV)) and durability (Slake Durability Index (SDI), Los Angeles Abrasion Value (LAAV), and Sulphate Soundness Value (SSV)). Uncrushed aggregates consisted exclusively of rounded particles because these were recycled from Upper Siwalik quartzite-dominant conglomerates. Samples were selected from each sampling site and further classified into bladed and equant shapes to assess whether form influences strength and durability.

Strength tests included PLSI, AIV, and ACV. The PLSI test followed the procedure outlined by ASTM D5731–02 (2002). The standard PLSI value (Is50) was converted to Uniaxial Compressive Strength (UCS) following ISRM (1981). For AIV and ACV tests, procedures from BS 812-112 (1990) and BS 812-110 (1990) were used, respectively.

Durability tests comprised SDI, LAAV, and SSV. The SDI test evaluates resistance to cyclic drying and wetting (Franklin & Chandra, 1972). It was performed in accordance with ASTM D4644-87 (2008), and the second-cycle SDI (Id2) was used to report the standard SDI. Samples after the second cycle were classified using Type 1, Type 2, and Type 3 degradation patterns. Gambles Slake Durability Classification (Goodman, 1980) was applied for SDI classification. A total of five test cycles were conducted to obtain deterioration characteristics. The LAAV test measures resistance to abrasion and impact, serving as an indirect measure of rock hardness. It was performed following ASTM C535 (2009) using Grade 2 test samples. The SSV test indicates resistance to cyclic freeze-thaw weathering and was conducted following ASTM C88–05 (2005).

All strength and durability tests were conducted on one test sample per sampling unit. The AIV, SDI, LAAV, and SSV tests were carried out at the Central Department of Geology, Tribhuvan University, while the PLSI test was performed at the Department of Mines and Geology, Ministry of Industry and Tourism, Kathmandu. The ACV test was conducted at the Institute of Engineering, Central Material Testing Laboratory (CMTL), Tribhuvan University.

4. Results

Characteristics of Quartzite Aggregates Samples

The quartzite aggregate samples from the Fagfog Quartzite area near Kalidaha Bazar towards Malekhu exhibit distinctive lithological and megascopic characteristics. These samples are classified as laminated, rippled, or massive, and medium-grained. They are very angular (VA), rough-textured, and yellowish-white to brownish-white quartzites. The Dunga Quartzite samples, predominantly located along road cut slopes of the Suparitar to Bhimpedi road section, display consistent lithological and megascopic features. These samples are categorized as very angular (VA), rough-textured, light grey to milky white quartzites, characterized by well-banded or crudely banded structures. The Pandrang Quartzite samples from the Suparitar to Bhimpedi road section are characterized by massive or laminated structures, fine-grained, bluish grey to grey, often exhibiting very angular and rough textures. The Chisapani Quartzite samples, located along the same section, exhibit laminated to massive, fine-grained, very angular rough textures, typically displaying grey with occasional bluish or greenish-grey hues. All the quartzite aggregates obtained from the bedrock belong to the Precambrian Era.

Two forms of samples, one bladed and one equant, were collected from each sampling locality in the Kamane-Chisapani area of the alluvial fan. The natural uncrushed quartzite samples are rounded with smooth surface textures. They are white to light grey quartzites belonging to the Post-Siwalik, i.e., Mid Pleistocene to Recent, and are deposited in the alluvial fan after being released and recycled from the conglomerate source rock of the Upper Siwalik.

Composition, Texture and Microstructure of Quartzite Under Polarizing Microscopes

Fagfog Quartzite

The Fagfog Quartzite samples, when examined under a polarizing microscope, show consistent composition and texture. The grains are subequant to elongate quartz grains that appear irregular, often showing long to sutured boundaries (Figure 3). The grain size distribution is broad, with minimum sizes averaging around 20 µm and maximum sizes extending up to 110 µm, with an average mode around 48–53 µm (Table 2). This variability suggests a diverse but generally medium-grained texture. Microstructurally, these quartzites display a massive appearance with undulose extinction, indicating wavy or curved grain boundaries.

DOI:https//doi.org/10.22452/mjs.vol44no3.4
Malaysian Journal of Science 44(3): 27-49 (September 2025)

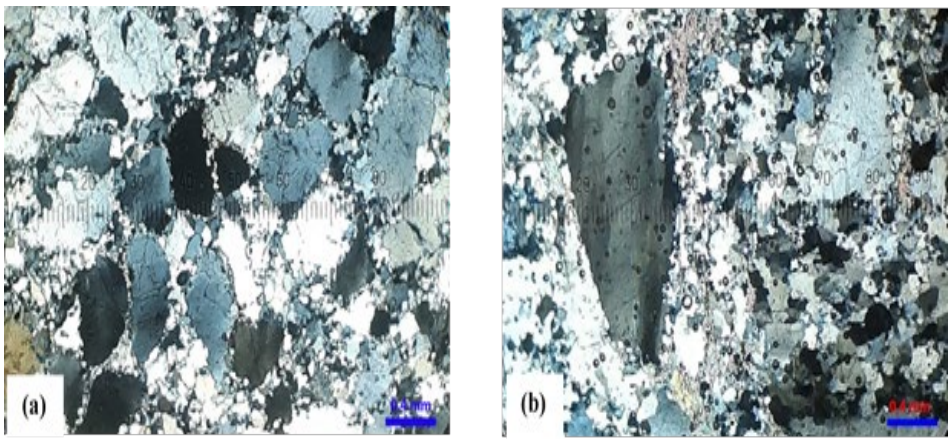

Figure 3. Photomicrographs of Quartzites under a polarizing microscope in crossed polars showing fabric and composition: (a) Fagfog Quartzite, and (b) Dunga Quartzite.

Table 2. Composition of quartzite of the samples

Stratig-raphic unit	Sample	*Quartz grain habit and fabric	Grain size (μ) Min	Max	Avg	Mode	*Microstructure	**Non mica/mica Band Ratio
Fagfog Quartzite	F1	subequant to elongate, irregular; long to sutured	30	70	48	40	Massive, undulosed, SGR	
	F2	subequant to elongate, irregular; long to sutured	20	90	52	40	Massive, undulosed, SGR	
	F3	subequant to elongate, irregular; long to sutured	20	70	41	30	Massive, undulosed, SGR	
	F4	subequant to elongate, irregular; long to sutured	30	90	47	50	Massive, undulosed, SGR	
	F5	subequant, irregular; sutured	30	100	52	40	Massive, undulosed, BGR with minor SGR	
	F6	subequant to elongate, irregular; long to sutured	20	70	44	40	Massive, undulosed,, BGR with minor SGR	
	F7	subequant to elongate, irregular; long to sutured	20	110	46	30	Massive, undulosed, SGR	
	F8	subequant to elongate, irregular; ; long to sutured	20	110	49	30	Massive, undulosed, minor BGR with SGR	
	F9	subequant to elongate, irregular; long to sutured	30	110	45	50	Massive, undulosed, SGR	
	F10	subequant to elongate, irregular; long to sutured	30	110	51	50	Massive, undulosed, BGR with SGR	
	F11	subequant to elongate, irregular; long to sutured	30	90	47	40	Massive, undulosed, SGR	
	F12	subequant to elongate, irregular; long to sutured	30	100	49	40	Massive, undulosed, SGR	
	F13	subequant to elongate, irregular; long to sutured	20	110	42	40	Massive, undulosed, SGR	
	F14	subequant to elongate, angular to subangular; irregular; long to sutured	30	90	43	30	Massive, undulosed, minor BGR with SGR	
	F15	subequant to elongate, long to sutured	30	110	53	40	Massive, undulosed, minor BGR with SGR	
Dunga Quartzite	D1	equigranular, straight to irregular, polygonal few suture and diffused	30	100	48	40	Mica: 0.025 mm (mode); Non mica: 0.175 mm (mode)	7

DOI:https//doi.org/10.22452/mjs.vol44no3.4
Malaysian Journal of Science 44(3): 27-49 (September 2025)

	D2	equigranular, straight to irregular, polygonal few suture and diffused	30	70	36	30	Mica: 0.020 mm; Non mica: 0.200 mm	10
	D3	equigranular, straight to irregular, polygonal few suture and diffused, few elongated grains	30	70	38	60	Mica: 0.020 mm; Non mica: 180 m	9
	D4	equigranular, small subgrain, equant subgrain, mostly irregular, and ameobodial	30	110	46	60	Mica: 0.015 mm; Non mica: 0.181 mm	10
	D5	equigranular, small subgrain, equant subgrain, mostly irregular, and ameobodial	30	90	41	40	Mica: 0.015 mm; Non mica: 0.100 mm	7
	D6	equigranular, small subgrain, equant subgrain, mostly irregular, and ameobodial	30	90	35	30	Mica: 0.030 mm; Non mica: 120 mm	4
	D7	equigranular, small subgrain, equant subgrain, mostly irregular, and ameobodial	20	60	39	40	Mica: 0.030 mm; Non mica: 0.080 mm	3
	D8	equigranular, small subgrain, equant subgrain, mostly irregular, ameobodial, and slightly diffused boundary	30	90	43	50	Mica: 0.030 mm; Non mica: 0.120 mm	4
	D9	dynamic recrystalization, small subgrain to large pophyro clast, with irregular boundaries, and ameobodial habit	30	130	80	60	Mica: 0.030 mm; Non mica: 0.275 mm	9
	D10	dynamic recrystalization, small subgrain to large pophyro clast, with irregular boundaries, ameobodial habbit, more elongated and lensolidal shape	30	110	57	40	Mica: 0.020 mm; Non mica: 150 mm	8
	D11	dynamic recrystalization with distinct folliation, equigranular, few lensolidal, irregular, and suture boundary	20	100	56	40	Mica: 0.035 mm; Non mica: 0.100 mm	3
	D12	equigranular, notable subgrain proportion nearby 50%, and irregular boundary	30	130	62	70	Mica: 0.030 mm; Non mica: 0.120 mm	4
	D13	slightly equigranular, irregular, suture, diffused grain boundary with few elongated grain	30	130	52	40	Mica: 0.015 mm; Non mica: 0.090 mm	6
	D14	equigranular, irregular suture, and diffused with few elongated grains.	20	70	42	30		
	D15	less equigranular, irregular diffuse, boundary among grains, and moreless subequant	30	130	61	40	Mica: 0.015 mm; Non mica: 0.100 mm	7
Pandrang Quartzite	P1	subequant, straight to irregular grain boundary	20	80	47	40	Mica: 0.010 mm; Non mica: 0.250 mm	25
	P2	subequant, few elongate, straight to irregular boundary	30	170	73	70	Mica: 0.030 mm; Non mica: 0.325 mm	11

DOI:https//doi.org/10.22452/mjs.vol44no3.4
Malaysian Journal of Science 44(3): 27-49 (September 2025)

P3	subequant, irregular to straight polygonal	20	150	64	70	Mica: 0.050 mm; Non mica: 0.350 mm	7
P4	subequant, irregular to straight polygonal	30	130	65	50	Mica: 0.020 mm; Non mica: 0.080 mm	4
P5	subequant, irregular to straight polygonal	30	90	53	40	Mica: 0.035 mm; Non mica: 0.100 mm	3
P6	subequant, irregular to straight polygonal	30	120	69	60	Mica: 0.025 mm; Non mica: 0.275 mm	11
P7	subequant, irregular to straight polygonal	30	110	64	50	Mica: 0.030 mm; Non mica: 0.160 mm	5
P8	subequant, irregular to straight polygonal	30	110	51	40	Mica: 0.015 mm; Non mica: 0.140 mm	9
P9	equigranular, equant, few elongate, straight to irregular	30	110	58	40	Mica: 0.015 mm; Non mica: 0.050 mm	3
P10	equigranular, subequant, elongate, straight to irregular	20	100	50	40	Mica: 0.040 mm; Non mica: 0.210 mm	5
P11	mostly equant, straight polygonal to irregular boundary	30	130	54	60	Mica: 0.055 mm; Non mica: 0.150 mm	3
P12	mostly equant, straight polygonal to irregular boundary	30	90	48	40	Mica: 0.040 mm; Non mica: 0.075 mm	2
P13	subequant, polygonal grains, mostly straight, few irregular	30	110	52	50	Mica: 0.050 mm; Non mica: 0.200 mm	4
P14	mostly subequant grains, polygonal, straight, few irregular	30	80	48	40	Mica: 0.050 mm; Non mica: 0.080 mm	1
P15	mostly subequant grains, polygonal, straight, few irregular	30	130	68	50	Mica: 0.020 mm; Non mica: 0.110 mm	6
C1	equigranular, subequant to elongate, straight to substraight	30	130	53	50	Mica: 0.020 mm; Non mica: 0.100 mm	5
C2	equigranular, subequant to elongate, straight to substraight, ribbon like	40	140	76	70	Mica: 0.030 mm; Non mica: 0.195 mm	7
C3	equigranular, subequant to elongate, straight to substraight, ribbon like	30	100	57	40	Mica: 0.030 mm; Non mica: 0.250 mm	8
C4	equigranular, subequant to elongate, straight to substraight, ribbon like	30	110	46	50	Mica: 0.030 mm; Non mica: 0.300 mm	8
C5	polygonal, three boundary junction	20	70	36	30	Mica: 0.050 mm; Non mica: 0.300 mm	6
C6	equigranular, subequant to elongate, ribbon like, straight to substraight, polygonal	30	130	60	40	Mica: 0.050 mm; Non mica: 0.250 mm	5
C7	equigranular, subequant to elongate ribbon like quartz, straight to substraight, polygonal	30	130	79	70	Mica: 0.020 mm; Non mica: 0.160 mm	8
C8	equigranular, subequant to elongate ribbon like quartz, straight to substraight, polygonal	30	110	56	40	Mica: 0.030 mm; Non mica: 0.130 mm	4
C9	equigranular, subequant to elongate ribbon like quartz,	30	110	58	50	Mica: 0.020 mm; Non mica: 0.210 mm	11

Chisapani Quartzite

DOI:https//doi.org/10.22452/mjs.vol44no3.4
Malaysian Journal of Science 44(3): 27-49 (September 2025)

	straight to substraight, polygonal						
C10	equigranular, subequant to elongate ribbon like quartz, straight to substraight, polygonal	40	110	76	80	Mica: 0.015 mm; Non mica: 0.220 mm	15
C11	equigranular, subequant to elongate, straight to substraight, polygonal	40	110	69	60	Mica: 0.015 mm; Non mica: 0.200 mm	13
C12	equigranular, subequant to elongate ribbon like quartz, straight to substraight, distinct polygonal	30	100	57	40	Mica: 0.015 mm; Non mica: 0.150 mm	10
C13	equigranular, subequant to elongate ribbon like quartz, straight to substraight, distinct polygonal	30	100	62	40	Mica: 0.030 mm; Non mica: 0.200 mm	7
C14	equigranular, subequant to elongate, straight to substraight, polygonal	30	110	58	90	Mica: 0.025 mm; Non mica: 0.150 mm	6
C15	more subequant than elongate, straight to substraight, distinct polygonal	30	130	77	70	Mica: 0.030 mm; Non mica: 0.200 mm	7
K1	inequigranular, subequant and elongate, intelocked, sutured	87	1200	338	200	Continuous foliation; Mica: 0.040 mm; Non mica: 0.400 mm	10
K2	inequigranular, subequant and elongate, intelocked, sutured	55	350	220	200	Massive, interlocked, sutured, BGR>SGR; grains 85% (0.3 mm), subgrains 15%	
K3	inequigranular, subequant and elongate, sutured	35	300	60	80	Continuous foliation; Mica: 0.010 mm; Non mica: 0.80 mm	8
K4	inequigranular, subequant and elongate, sutured	75	900	259	400	Massive, interlocked, BGR>SGR; Grains 85% (0.8 mm), subgrains 15%	
K5	subequigranular, subequant and elongate, interlocked, sutured	20	300	100	150	Continuous foliation; Mica: 0.010 mm; Non mica: 0.080 mm	8
K6	inequigranular, subequant and elongate, sutured	17	1900	400	450	Massive, interlocked, sutured, SGR with few BGR; grains 80% (0.8 mm), subgrains 20%	
K7	subequigranular, subequant and elongate, interlocked, sutured	20	300	160	200	Continuous foliation; Mica: 0.005 mm; Non mica: 0.200 mm	40
K8	subequigranular, subequant and elongate, recrystallized	20	400	210	180	Mica: 0.005 mm; Non mica: 0. 200 mm	40
A1	inequigranular, subequant and elongate	47	2000	208	400	Massive, interlocked, wavy foliation, BGR >SGR; grain 85% (0.4 mm), subgrain 15%	
A2	subequigranular, subequant and elongate, amoeboid	173	800	384	600	Massive, interlocked, Grains with wavy foliation, grains 85% (0.5 mm), subgrains 15%	
A3	subequigranular, sutured, well siliceous cemented	45	1200	456	610	Massive, interlocked, orthoquartzite; grains 90% (0.5 mm), subgrains 10%	
A4	subequigranular, elongate, irregular boundaries	60	400	144	215	Continuous foliation; Mica: 0.010 mm; Non mica: 0,100 mm	10

Alluvial Fan Gravel

DOI:https//doi.org/10.22452/mjs.vol44no3.4
Malaysian Journal of Science 44(3): 27-49 (September 2025)

G1	subequigranular, mostly elongate, straight to irregular boundaries	90	495	265	380	Continuos foliation; Mica: 0.010 mm; Non mica: 0.100 mm	10
G2	inequigranular, subequant and elongate, sutured	60	830	315	330	Massive, interlocked, sutured, BGR >SGR; grains 80% (0.3 mm); subgrains 20%	
C1	inequigranular, subequant and elongate, intelocked, sutured	50	800	212	275	Massive, interlocked, sutured, BGR>SGR; grains 85% (0.2 mm); subgrains 15%	

*Microstucture: BLG=buldging grain recrystallization; SGR=sediment grain rotation

**Band Ratio = Mode of Non-mica thickness/Mode of mica thickness

Dunga Quartzite

The Dunga Quartzite samples exhibit distinct characteristics in composition, texture, and microstructure (Table 2). They are primarily equigranular, with grains varying from straight to irregular, often displaying polygonal shapes with occasional sutured boundaries (Figure 3). Grain sizes range widely from 20 µm to 130 µm, averaging between 35 µm and 80 µm. Microstructurally, these quartzites show small subgrains and equant subgrains, indicating dynamic recrystallization processes. Some samples present irregular and amoeboidal grain boundaries, suggesting varying degrees of deformation and metamorphism. Mica bands range slightly but generally fall between 0.015 mm and 0.035 mm, with non-mica bands varying from 0.080 mm to 0.275 mm. The band ratio of non-mica to mica spans from 3 to 10 and is notably higher in some samples, indicating different degrees of metamorphic activity and recrystallization.

Pandrang Quartzite

Quartz grains are generally equigranular and predominantly subequant, with boundaries ranging from straight to irregular in shape (Figure 4). Grain sizes vary significantly, from 20 µm to 170 µm, averaging between 47 µm and 73 µm across different samples (Table 2). Microscopically, the quartz grains exhibit polygonal shapes with mainly straight boundaries, suggesting relatively stable crystallization conditions. Some samples contain elongated grains, indicating possible deformation during formation. Mica bands in these quartzites range from 0.010 mm to 0.055 mm, while non-mica bands vary from 0.050 mm to 0.350 mm. The non-mica to mica band ratio ranges from 1 to 25, reflecting varying conditions of alternating banding between mica and non-mica components in the rock.

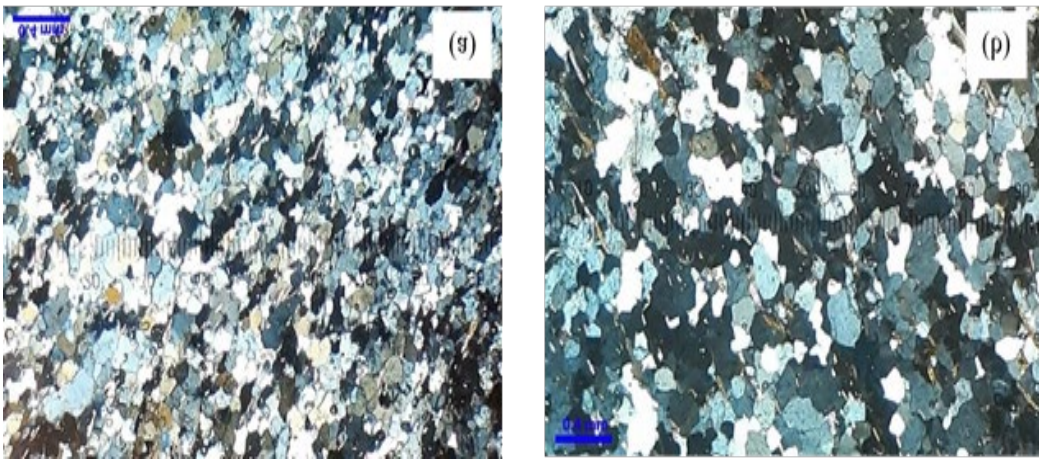

Figure 4. Photomicrographs of quartzites under a polarizing microscope. (a) Pandrang Quartzite and (b) Chisapani Quartzite.

Chisapani Quartzite

The Chisapani Quartzite samples exhibit a consistent pattern of equigranular texture with grains ranging from subequant to elongate shapes under the polarizing microscope (Figure 4). Grain sizes vary from a minimum of 20 µm to a maximum of 140 µm, with an average size between 36 µm and 79 µm across different samples. The modal grain size typically falls between 30 µm and 80 µm. Quartzites display straight to substraight boundaries, with some samples showing ribbon-like structures, indicating potential flow patterns during formation (Table 2; Figure 4). Mica band thickness ranges from 0.015 mm to 0.050 mm, with non-mica components varying from 0.100 to 0.300 mm. The non-mica to

DOI:https//doi.org/10.22452/mjs.vol44no3.4
Malaysian Journal of Science 44(3): 27-49 (September 2025)

mica band ratio varies from 5 to 15. The polygonal grain boundaries are well defined in most samples, suggesting relatively stable crystallization conditions.

Uncrushed Quartzite

The Alluvial Fan Gravel quartzites, as observed under the polarizing microscope, display a range of distinct features. These samples are characterized by an inequigranular texture with grains varying from subequant to elongate shapes, often interlocked and exhibiting sutured boundaries. Grain sizes across samples range widely, from 17 µm to 1900 µm, with an average size between 60 µm and 400 µm, and a mode typically around 200 µm.

Microscopically, these quartzites exhibit continuous foliation patterns, indicating significant deformation and recrystallization during metamorphism. The presence of mica, ranging from 0.005 mm to 0.050 mm, reflects varying degrees of metamorphic activity affecting mineral composition. The non-mica to mica band ratio is notably high in some samples, indicating intense metamorphism and recrystallization processes (Table 2; Figure 5).

Figure 5. Photomicrographs of natural quartzites gravel under a polarizing microscope. (a) Sample k8 shows polygonal quartz of interlocked and metamorphic recrystallization (quartzite), and (b) Sample A3 shows rounded to subrounded quartz, cemented.

Overall, the Alluvial Fan Gravel quartzites demonstrate their geological significance through their intricate microfabric characteristics, which provide insights into their formation conditions and metamorphic history. The interlocked and sutured grain boundaries, along with the foliation patterns, emphasize the dynamic geological processes these rocks have experienced. Such features make these quartzites valuable for understanding their potential applications in geotechnical engineering and construction.

Strength and Durability of quartzite

Point Load Strength Index (PLSI)

The ranges of PLSI values for the Fagfog Quartzite, Dunga Quartzite, Pandrang Quartzite, and Chispani Quartzite samples are 2.40–3.02 MPa, 3.68–13.77 MPa, 3.68–13.77 MPa, and 0.53–7.31 MPa, respectively (Table 3). Based on the UCS values (Table 3), the Fagfog Quartzite samples predominantly fall within the strong to extreme categories. Among the Dunga Quartzite samples, 60 percent fall within the very strong category, thirty-three percent within the strong category, and the remainder in the medium strong category. Several Pandrang Quartzite samples are classified as very strong to strong (Table 3). For the Chispani Quartzite samples, several are categorized as very strong, with a few classified as strong and medium strong. Overall, the PLSI values offer valuable insights into the strength characteristics of the Chispani Quartzite ballasts.

The PLSI for the rounded (uncrushed) ballast samples ranges from 8.07 to 13.53 MPa. Most of the rounded pebble quartzite ballast samples fall within the very strong and strong categories. Among these samples, sixty-six percent are classified as very strong.

DOI:https//doi.org/10.22452/mjs.vol44no3.4
Malaysian Journal of Science 44(3): 27-49 (September 2025)

Table 3. Strength parameters of Quartzite aggregates

Stratigraphic Unit	Sample	Is(50), Mpa	UCS, Mpa	*Remarks	AIV (%)	ACV (%)
Fagfog Quartzite	F1	6.82	177	VS	17	22
	F2	4.93	137	VS	19	21
	F3	4.70	94	S	19	20
	F4	3.07	62	S	17	22
	F5	8.15	213	VS	23	16
	F6	4.52	67	S	15	17
	F7	2.40	39	MS	18	20
	F8	4.18	85	S	17	23
	F9	6.02	119	VS	20	30
	F10	3.48	80	S	18	22
	F11	6.66	155	VS	18	21
	F12	4.23	144	VS	17	22
	F13	11.55	302	ES	15	20
	F14	2.93	85	S	21	21
	F15	5.42	145	VS	22	20
Dunga Quartzite	D1	5.97	177	VS	17	26
	D2	4.26	97	S	22	26
	D3	3.68	94	S	18	24
	D4	6.94	94	S	20	25
	D5	5.11	94	S	22	28
	D6	5.84	138	VS	16	25
	D7	5.11	97	S	28	31
	D8	3.77	94	S	19	31
	D9	5.11	101	VS	17	27
	D10	9.43	251	ES	12	21
	D11	4.68	137	VS	15	22
	D12	13.77	297	ES	10	18
	D13	8.26	226	ES	14	29
	D14	9.30	133	VS	14	21
	D15	8.34	163	VS	15	20
Pandrang Quartzite	P1	4.31	207	VS	15	22
	P2	1.91	92	S	24	28
	P3	3.48	167	VS	17	25
	P4	2.03	97	S	20	25
	P5	3.20	154	VS	16	25
	P6	1.46	70	S	17	24
	P7	2.15	103	VS	18	25
	P8	2.50	120	VS	18	22
	P9	1.49	71	S	13	22
	P10	1.99	95	S	13	21
	P11	2.74	132	VS	21	22
	P12	2.61	125	VS	20	23
	P13	1.75	84	S	17	24
	P14	2.50	120	VS	23	30
	P15	3.15	151	VS	20	29

Stratigraphic Unit	Sample	Is(50), Mpa	UCS, Mpa	*Remarks	AIV (%)	ACV (%)
Chisapani Quartzite	C1	2.97	143	VS	18	22
	C2	2.07	99	S	19	28
	C3	3.38	162	VS	20	25
	C4	7.02	337	ES	14	25
	C5	3.43	164	VS	19	25
	C6	3.60	173	VS	24	24
	C7	2.03	97	S	26	25
	C8	1.83	88	S	23	22
	C9	2.18	105	VS	15	22
	C10	2.18	105	VS	33	21
	C11	2.47	119	VS	23	22
	C12	0.53	25	MS	33	23
	C13	2.06	99	S	22	24
	C14	0.81	39	MS	26	30
	C15	2.60	125	VS	34	29
Alluvial Fan Gravel	K1	1.84	88	VS	22	22
	K2	2.20	106	S	19	20
	K3	2.70	130	VS	21	20
	K4	2.21	106	S	24	20
	K5	1.85	89	VS	19	18
	K6	2.29	110	S	19	21
	K7	3.02	145	VS	22	21
	K8	2.59	124	VS	23	26
	A1	2.11	101	S	21	21
	A2	2.13	102	S	23	36
	A3	1.84	88	VS	23	20
	A4	1.71	82	VS	21	24
	G1	3.86	185	S	20	24
	G2	3.08	148	VS	24	20
	C1	2.33	112	VS	22	23

*ISRM (1981): 0.25-1 MPa= extremely weak; 1-5.0 MPa= very weak; 5.0-25 MPa = weak (W); 25-50 MPa= medium strong rock (MS); 50-100 MPa= strong (S); 100-250 MPa= very strong (VS); >250 MPa extremely strong (ES)

DOI:https//doi.org/10.22452/mjs.vol44no3.4
Malaysian Journal of Science 44(3): 27-49 (September 2025)

Aggregate Impact Value (AIV) and Aggregate Crushing Value (ACV)

The ranges of the AIV for the Fagfog Quartzite, Dunga Quartzite, Pandrang Quartzite, and Chisapani Quartzite samples (Table 3) are 15–23%, 10–28%, 13–24%, and 18–33%, respectively. The ranges of the ACV for the Fagfog Quartzite, Dunga Quartzite, Pandrang Quartzite, and Chisapani Quartzite samples (Table 3) are 16–30%, 18–31%, 21–30%, and 21–30%, respectively. Considering AIV and ACV results for all the crushed rock samples, the AIV ranges from 10% to 33%, and ACV from 16% to 31%. Samples from the Fagfog Quartzite and the Pandrang Quartzite exhibit narrower ranges of impact strength, with results superior to those from the Dunga Quartzite and Chisapani Quartzite. The crushing strength of all samples from the four stratigraphic units falls within a similar range, demonstrating consistent results.

For uncrushed natural gravels, the AIV ranges from 19% to 24%, and ACV ranges from 18% to 36% (Table 3). Sixty-six percent of samples exhibit AIV between 19% and 22%, with the remainder up to 24%. Similarly, sixty-six percent of samples show ACV between 18% and 22%, while the remaining 26% range from 23% to 26%. The results for both impact and crushing strength in uncrushed natural gravel indicate promising quality.

Slake Durability Index (SDI)

In the SDI 2nd cycle (Id2), the majority of Fagfog samples demonstrate very high durability according to Gamble's Slake Durability Classification (Goodman, 1980), with percentages exceeding 98% (Table 4). Approximately 10% of samples show a reduction from very high to high durability by the fifth cycle. All Dunga Quartzite samples show Id2 values indicating very high durability, exceeding 98%, reflecting their resistance to slaking. Notably, about 33% of these samples maintain a perfect SDI of 100%, demonstrating exceptional resilience. The Pandrang Quartzite samples exhibit remarkable durability up to the fifth cycle, with all samples showing very high durability (98%–100%) at the second cycle. Moreover, 25% of these samples retain 100% durability, underscoring their exceptional resistance to slaking. The SDI of the Chisapani Quartzite samples remains consistent between the second and fifth cycles; all samples exhibit very high durability at the second cycle, and the majority maintain this level at the fifth cycle, with minor fluctuations in some samples. Across all crushed rock samples, the SDI Id2 remains between 97% and 100%, and all samples display type I degradation. The SDI results indicate consistently high durability throughout the testing process.

For uncrushed natural gravels, Id2 values of bladed samples range from 99.56% to 100%, while those of equant samples range from 99.36% to 100%. After the fifth cycle, Id5 values for bladed samples range from 99.52% to 100%, and for equant samples from 99.36% to 99.86%. Uncrushed samples of both bladed and equant types therefore maintain very high durability even after the fifth cycle, confirming their resistance to slake weathering.

Table 4. Durability parameters of quartzite

		Slake Durability Index						LAAV (%)	SSV (%)
Unit	Sample	Initial Oven-dry wt. (g)	*Id_{1st} (%)	*Id_{2nd} (%)	*Id_{3rd} (%)	*Id_{4th} (%)	Id_{5th} (%)		
Fagfog Quartzite	F1	565	98.23	98.23	98.23	98.23	98.23	26.57	0.20
	F2	505	99.01	99.01	99.01	99.01	99.01	31.34	1.03
	F3	530	100.00	97.17	97.17	97.17	97.17	21.94	0.25
	F4	565	99.12	99.12	99.12	98.23	98.23	17.47	0.60
	F5	525	100.00	100.00	99.05	98.10	98.10	28.24	4.59
	F6	490	97.96	96.94	96.94	95.92	95.92	21.38	0.25
	F7	520	98.08	97.12	97.12	97.12	95.19	12.07	1.47
	F8	555	99.10	98.20	98.20	95.50	95.50	29.17	0.95
	F9	560	99.11	99.11	99.11	99.11	99.11	29.30	1.99
	F10	510	100.00	100.00	100.00	100.00	99.02	26.23	1.98
	F11	490	98.98	98.98	98.98	98.98	98.98	25.18	1.95
	F12	470	100.00	98.94	98.94	98.94	98.94	22.89	1.23
	F13	530	100.00	99.06	99.06	99.06	99.06	17.12	4.18
	F14	490	100.00	100.00	98.98	98.98	98.98	15.52	2.19
	F15	520	99.04	99.04	99.04	99.04	99.04	29.38	2.91
Dunga Quartzite	D1	515	98.06	98.06	97.09	97.09	97.09	16.90	0.05
	D2	545	100.00	99.08	99.08	99.08	99.08	22.79	0.48
	D3	510	100.00	100.00	100.00	100.00	100.00	29.04	0.24
	D4	555	99.10	99.10	99.10	99.10	99.10	16.05	0.24
	D5	510	100.00	100.00	100.00	100.00	100.00	27.55	0.10
	D6	545	100.00	100.00	100.00	99.08	99.08	23.78	0.10
	D7	505	99.01	99.01	99.01	98.02	98.02	31.32	0.15
	D8	545	99.08	99.08	99.08	98.17	98.17	24.09	0.10
	D9	540	99.07	99.07	98.15	98.15	98.15	28.85	0.14

DOI:https//doi.org/10.22452/mjs.vol44no3.4
Malaysian Journal of Science 44(3): 27-49 (September 2025)

Pandrang Quartzite	D10	510	99.02	99.02	99.02	99.02	99.02	17.70	0.00
	D11	555	100.00	99.10	99.10	99.10	99.10	27.08	0.24
	D12	520	100.00	100.00	99.04	99.04	99.04	15.42	0.00
	D13	530	100.00	100.00	100.00	100.00	100.00	14.89	0.20
	D14	520	100.00	99.04	99.04	99.04	99.04	17.20	0.25
	D15	520	99.04	99.04	99.04	99.04	99.04	18.41	0.25
	P1	505	100.00	100.00	100.00	100.00	100.00	15.85	0.00
	P2	545	99.08	99.08	99.08	98.17	98.17	24.38	0.00
	P3	525	100.00	100.00	100.00	99.05	99.05	27.87	0.00
	P4	505	100.00	99.01	99.01	99.01	99.01	27.67	0.00
	P5	505	100.00	100.00	100.00	99.01	99.01	24.08	0.00
	P6	555	99.10	99.10	98.20	98.20	98.20	32.49	0.00
	P7	550	99.09	99.09	99.09	99.09	98.18	31.31	0.00
	P8	555	100.00	100.00	99.10	99.10	99.10	23.72	0.00
	P9	505	99.01	99.01	99.01	99.01	99.01	29.97	0.00
	P10	550	100.00	100.00	100.00	99.09	99.09	22.78	0.00
	P11	545	99.08	98.17	98.17	98.17	98.17	23.08	0.24
	P12	545	100.00	99.08	99.08	99.08	99.08	33.91	0.25
	P13	555	99.10	99.10	99.10	99.10	99.10	37.17	0.00
	P14	560	99.11	99.11	99.11	99.11	98.21	28.41	0.00
	P15	545	99.08	99.08	99.08	98.17	98.17	24.38	0.00

* Gambles Slake Durability Classification (Goodman, 1980): I2nd: >98% very high durability; 95-98% high durability; 85-95 medium high durability; 60-85 medium durability; 30-60 low durability; <30 very low durability; a = bladed samples; b = equant samples

Unit	Sample	Slake Durability Index: Initial Oven-dry wt. (g)	*Id_{1st} (%)	*Id_{2nd} (%)	*Id_{3rd} (%)	*Id_{4th} (%)	Id_{5th} (%)	LAAV (%)	SSV (%)
Chisapani Quartzite	C1	550	100.00	99.09	99.09	99.09	99.09	25.53	0.25
	C2	525	100.00	99.05	99.05	99.05	99.05	32.11	0.00
	C3	570	99.12	98.25	98.25	98.25	98.25	31.50	0.74
	C4	540	100.00	100.00	100.00	100.00	100.00	22.35	0.00
	C5	505	99.01	99.01	99.01	99.01	98.02	23.80	0.00
	C6	520	99.04	99.04	99.04	99.04	98.08	32.84	0.00
	C7	520	99.04	99.04	99.04	99.04	99.04	33.87	0.00
	C8	530	100.00	100.00	99.06	99.06	99.06	44.36	0.00
	C9	535	99.07	99.07	99.07	99.07	99.07	22.58	0.00
	C10	585	99.15	99.15	98.29	98.29	98.29	41.75	0.00
	C11	530	100.00	100.00	99.06	99.06	99.06	44.64	0.00
	C12	535	99.07	98.13	97.20	97.20	97.20	48.63	0.48
	C13	530	100.00	99.06	99.06	99.06	98.11	33.25	0.00
	C14	540	100.00	99.07	99.07	99.07	98.15	41.12	0.00
	C15	545	98.17	98.17	98.17	97.25	97.25	47.98	0.25
Alluvial Fan Gravel	K1a	648	100.00	100.00	100.00	100.00	100.00	28.15	0.05
	K2a	755	99.87	99.87	99.87	99.74	99.74	28.87	0.05
	K3a	598	100.00	100.00	100.00	99.83	99.83	30.72	0.15
	K4a	599	100.00	99.83	99.83	99.83	99.83	30.38	0.25
	K5a	628	100.00	100.00	100.00	100.00	99.84	28.20	0.10
	K6a	450	99.78	99.56	99.56	99.56	99.56	34.28	0.14
	K7a	751	99.87	99.73	99.73	99.73	99.73	26.97	0.00
	K8a	698	100.00	100.00	100.00	100.00	100.00	31.19	0.00
	A1a	540	100.00	100.00	100.00	100.00	99.81	30.12	0.39
	A2a	785	100.00	99.87	99.87	99.87	99.87	32.00	0.15
	A3a	735	100.00	99.86	99.86	99.86	99.73	35.48	0.29
	A4a	677	100.00	99.85	99.85	99.85	99.85	29.74	0.19
	G1a	672	100.00	100.00	100.00	100.00	99.85	33.66	0.14

DOI:https//doi.org/10.22452/mjs.vol44no3.4
Malaysian Journal of Science 44(3): 27-49 (September 2025)

G2a	627	99.84	99.68	99.68	99.52	99.52	34.10	0.05
C1a	714	99.86	99.72	99.72	99.72	99.58	36.40	0.10
K1b	642	100.00	99.84	99.84	99.84	99.84	28.44	0.00
K2b	624	99.84	99.68	99.52	99.52	99.36	24.89	0.15
K3b	631	99.84	99.84	99.84	99.84	99.68	27.87	0.00
K4b	686	100.00	100.00	100.00	99.85	99.85	31.13	0.29
K5b	643	99.84	99.84	99.84	99.69	99.53	31.03	0.34
K6b	403	100.00	100.00	99.75	99.75	99.75	30.31	0.10
K7b	647	100.00	99.85	99.69	99.69	99.54	28.09	0.25
K8b	710	100.00	100.00	100.00	99.86	99.86	33.46	0.25
A1b	634	100.00	100.00	100.00	100.00	99.84	26.81	0.00
A2b	751	100.00	100.00	99.87	99.87	99.73	28.43	0.32
A3b	693	100.00	100.00	100.00	99.86	99.86	39.98	0.10
A4b	674	100.00	100.00	99.85	99.70	99.70	29.82	0.10
G1b	697	99.86	99.86	99.86	99.71	99.57	32.56	0.20
G2b	570	100.00	100.00	99.82	99.65	99.65	35.36	0.00
C1b	745	99.73	99.73	99.60	99.46	99.46	31.13	0.29

* Gambles Slake Durability Classification (Goodman, 1980): I2nd: >98% very high durability;
95-98% high durability; 85-95 medium high durability; 60-85 medium durability;
30-60ow durability; <30 very low durability; a = bladed samples; b = equant samples

Los Angeles Abrasion Value (LAAV)

The LAAV of the Fagfog Quartzite samples ranges from 12.07 to 31.34% (Table 4). The LAAV ranges for Dunga Quartzite, Pandrang Quartzite, and Chisapani Quartzite are 14.89–31.32%, 25.53–44.64%, and 24.89–35.36%, respectively. The samples from Fagfog and Dunga Quartzite show a wider range of values compared to the Pandrang and Chisapani Quartzite samples. The narrowest range of LAAV is observed in the Chisapani Quartzite. These abrasion values indicate the resistance of the quartzite ballasts to wear, with lower values signifying higher durability.

The uncrushed bladed samples exhibit a LAAV range of 26.97–36.4%, while equant samples show LAAV from 24.89 to 39.98%. Approximately 10% of samples exceed 35% LAAV in both bladed and equant tests. These results demonstrate very good soundness of uncrushed gravel against abrasion and impact.

Sulphate Soundness Value (SSV)

The SSV of the Fagfog Quartzite samples varies from 0.2% to 4.59%, indicating relatively minor weight loss. Only 10% of samples exceed 4%, while most display losses below 2%. The Dunga Quartzite samples exhibit SSV between 0.05% and 0.48%, reflecting negligible degradation. Similarly, Pandrang and Chisapani Quartzite samples yield SSV ranges of 0–0.25% and 0–0.74%, respectively. Consequently, the crushed rock samples show a narrow and low range of SSV. These results provide insights into aggregate durability and stability under freeze-thaw weathering.

For uncrushed natural gravels, both bladed and equant samples have SSVs of 0.05–0.39% and 0–0.34%, respectively, which are low and narrowly distributed. These soundness values indicate the resistance of quartzite aggregates to sulfate-induced disintegration, with lower values signifying greater durability against sulfate attack and freeze-thaw cycles.

5. Discussion

Effect of Shape on Point Load Strength Index (PLSI)

Fagfog and Chisapani Quartzites exhibit higher maximum strengths, whereas Dunga and Pandrang Quartzites show consistent interlocking effects with moderate PLSI ranges. The interaction of shape, texture, and structure among these units underscores the complex relationship between morphology and mechanical strength in quartzite materials. Samples from all four quartzite units demonstrate that particle shape significantly affects PLSI values through interlocking and void formation. Aggregate particle shape also influences UCS due to factors including interlocking, packing density, and stress distribution, as noted by Štambuk Cvitanović et al. (2015).

Irregularly shaped particles may pack less efficiently than well-rounded ones, creating voids and weak zones within the material. This uneven packing can reduce UCS (Fairhurst & Hudson, 1999). Particle shape affects void volume and distribution; irregular shapes tend to generate more voids, weakening the structure and decreasing UCS. Conversely, well-graded aggregates with more uniform shapes minimize void content and enhance strength (Hoskins & Horino, 1968).

Crushed quartzite particles are highly angular, ranging from bladed to equant shapes, and exhibit rough textures. These characteristics strongly influence PLSI, which varies from 0.53 MPa to 7.02 MPa across stratigraphic units (Table 5; Figure 6). Angular particles promote interlocking, increasing mechanical stability and strength, as indicated by higher PLSI in well-interlocked samples. However, pronounced angularity can also induce voids or stress concentration points, resulting in lower PLSI in samples with greater porosity or weaker zones. In contrast, uncrushed quartzite

DOI:https//doi.org/10.22452/mjs.vol44no3.4
Malaysian Journal of Science 44(3): 27-49 (September 2025)

samples from alluvial gravels have PLSI values between 1.71 MPa and 3.86 MPa, generally classified as “very strong” or “strong.” These samples are predominantly subrounded with smooth textures. Subrounded particles have smoother surfaces and fewer sharp edges, which reduces interlocking and frictional resistance but also lowers stress concentration. This yields slightly lower strength than angular particles but maintains relatively high and consistent PLSI values due to uniform packing and stress distribution.

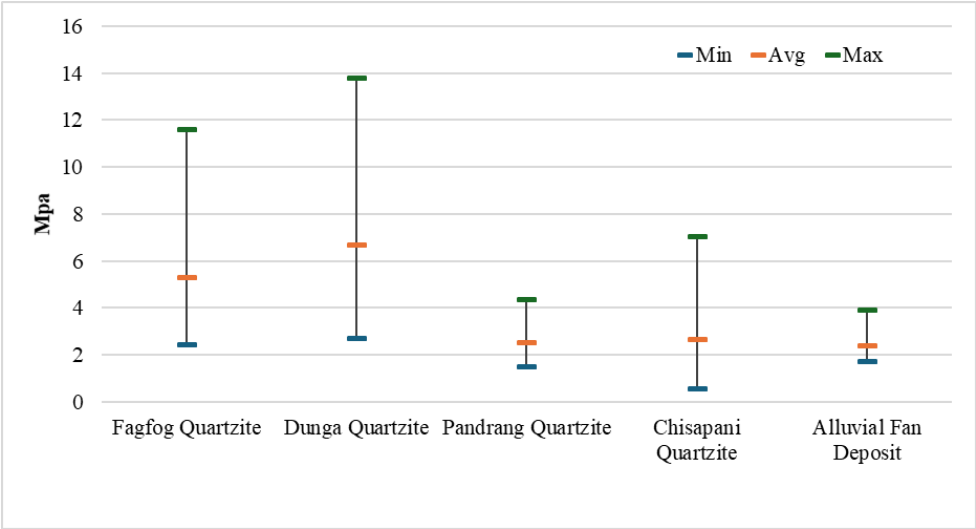

Figure 6. Variation of PLSI among crushed (angular) and uncrushed (rounded) samples

The graph shows a general trend of higher variability in PLSI values within units such as Dunga and Fagfog compared to the Pandrang Quartzite and Chisapani Quartzite. The strength of quartzite samples, as measured by the Point Load Strength Index, varies significantly across different stratigraphic units. The highest strength is observed in certain samples from the Fagfog and Dunga units, while the Pandrang and Chisapani Quartzite generally exhibit lower strength. The variations in PLSI values emphasize the importance of sample-specific and unit-specific characteristics in determining the strength properties of quartzite. Overall, the uncrushed, rounded, and smooth gravel subjected to point load testing exhibits lower and narrower ranges of PLSI compared to the higher and broader range yielded by the uncrushed angular samples. The shape of aggregate rocks influences stress distribution within the material during loading. Irregular shapes may concentrate stress at specific points, causing localized failure and reducing overall strength. Conversely, uniformly shaped aggregates distribute stress more evenly, resulting in higher UCS values (Podnicks et al., 1968). The surface roughness and irregularities of aggregate particles can also affect the UCS of the material (Richardson, 1991).

Effect of Shape on Aggregate Impact Value (AIV) and Aggregate Crushing Value (ACV)

The morphology of quartzite particles markedly impacts the AIV and ACV. Highly angular particles possess numerous sharp edges and corners that improve interparticle interlocking. This interlocking typically enhances resistance to impact and crushing forces, potentially yielding higher strength values. Some samples exhibit lower impact resistance but greater crushing resistance than others, suggesting that although these samples may not endure sudden impact well (due to effective interlocking), they can adjust packing and sustain compressive loads. Conversely, other samples show the opposite trend, indicating that internal weaknesses may more strongly influence their crushing performance. The Dunga Quartzite samples with lower AIV and ACV values demonstrate how finer or more uniform particle morphology can reduce susceptibility to fragmentation and impact damage. However, some Dunga Quartzite samples present high values of both AIV and ACV, reflecting inherent variability in the rock's composition and fabric. Similarly, Pandrang and Chisapani Quartzite samples display both elevated and reduced AIV and ACV values due to differences in angularity, texture, and geological characteristics, which substantially govern the aggregate’s mechanical behavior affecting AIV and ACV.

The morphology of quartzite particles critically influences the Aggregate Impact Value (AIV) and Aggregate Crushing Value (ACV), with marked differences among the Fagfog, Dunga, Pandrang, and Chisapani quartzites. Fagfog Quartzite samples exhibit highly angular shapes that enhance interlocking. Dunga quartzite samples, characterized by lower AIV and ACV values, reflect effective interlocking and uniform particle morphology, resulting in diminished fragmentation. Similar trends are observed in Pandrang quartzite. Chisapani quartzite samples also conform to these patterns.

The morphology of uncrushed quartzite particles, classified as subrounded with bladed to equant forms, considerably influences the AIV and ACV results. Subrounded particles generally have smoother surfaces and fewer sharp edges,

DOI:https//doi.org/10.22452/mjs.vol44no3.4
Malaysian Journal of Science 44(3): 27-49 (September 2025)

leading to diminished interlocking compared to more angular forms. This attribute usually results in moderate AIV and ACV values. For instance, samples K1 and K8 exhibit AIV values ranging from 18.63% to 23.53%, indicating reasonable resistance to impact forces, while their ACV values denote a comparable moderate performance under compressive loading. The consistent smooth texture across samples contributes to a uniform mechanical response, reflecting the intrinsic properties of alluvial gravel. However, some samples, such as A2, demonstrate higher ACV values (35.66%), implying that, despite their subrounded morphology, variations in internal structure or mineralogy affect overall strength.

Apparent distinctions arise between crushed quartzite (Fagfog, Dunga, Pandrang, Chisapani) and uncrushed quartzite. Crushed quartzite samples typically display highly angular shapes, enhancing interlocking and increasing resistance to impact and crushing forces. In contrast, uncrushed quartzite particles are predominantly subrounded, featuring smoother surfaces and fewer sharp edges. This results in reduced interlocking and moderate AIV and ACV values, as observed in samples exhibiting intermediate AIV. The uniform texture of uncrushed samples contributes to consistent mechanical performance, although some, such as A2 with an ACV of 35.66%, suggest compositional heterogeneity affecting strength.

Variations in aggregate impact and crushing values are governed by particle morphology and geological factors including bulk composition, grain size, texture, and weathering. According to Dhir et al. (1971) and Ramsay et al. (1974), elevated Aggregate Crushing Values observed in migmatite gneiss and porphyritic granite correspond to their texture and grain size. The Aggregate Impact Value (AIV) test provides a relative measure of aggregate resistance to sudden shock or impact, demonstrating high reproducibility and serving as a reliable mechanical parameter for aggregate evaluation (Al-Harthi, 2001; Smith & Collis, 2001).

The morphology of rock aggregates significantly influences their resistance to mechanical stresses. Irregular or elongated particles may induce stress concentrations and weaker interlocking, resulting in lower AIV values. Conversely, rounder or cuboidal particles distribute impact forces more evenly, affording higher AIV values (Afolagboye et al., 2016). Similarly, flaky or irregular shapes exhibit greater susceptibility to crushing under compressive loads, whereas cuboidal or equidimensional particles better withstand compressive forces, yielding higher ACV values (Afolagboye et al., 2016).

The significance of aggregate morphology on strength properties is further emphasized by Kuna and Bögöly (2024), who highlight its role in resistance to mechanical weathering and degradation. Their findings underscore the influence of shape on the strength characteristics of construction materials (Kuna & Bögöly, 2024). Aggregate morphology and texture substantially affect performance regarding strength and durability. Specifically, angular and rough-textured aggregates tend to interlock more effectively and resist impact and crushing forces better than rounded and smooth aggregates (Lees & Kennedy, 1975; Kazi & Al-Mansour, 1980).

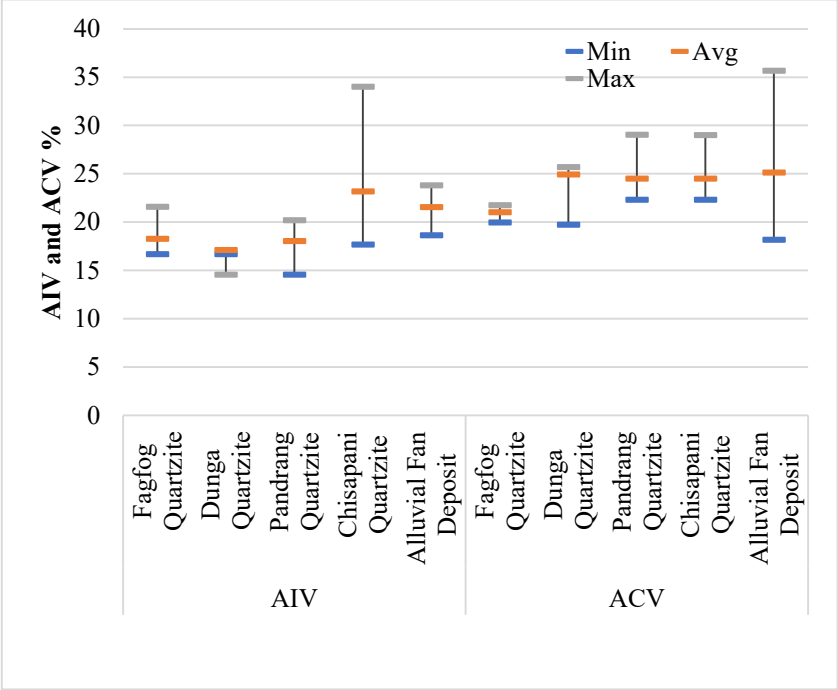

Figure 7. Variation of AIV and ACV among the crushed (angular, rough) and uncrushed (rounded smooth) samples

DOI:https//doi.org/10.22452/mjs.vol44no3.4
Malaysian Journal of Science 44(3): 27-49 (September 2025)

Effect of Shape on Slake Durability Index (SDI)

Slake durability indices across different cycles were determined for crushed and uncrushed quartzites. The Fagfog Quartzite samples are uniformly classified as very angular (VA) and range from bladed to prolate. Their surface textures are rough. The slake durability test shows variations in the second cycle Id2 and fifth cycle Id5 indices.

The shape of the quartzite samples plays a pivotal role in influencing these durability indices. Very angular shapes expose more surface area to weathering processes compared to more rounded shapes. This increased surface area can lead to greater susceptibility to mechanical breakdown during the slake durability tests. However, the high Id2 and Id5 values indicate that despite their very angular shapes, the quartzite samples exhibit substantial resistance to disintegration. This resistance can be attributed to the inherent hardness and interlocking grain structure characteristic of quartzite, which enhances its durability.

The Dunga Quartzite samples share similar megascopic descriptions and shapes, showing consistently high slake durability indices. All samples are described as very angular (VA), ranging from bladed to prolate, with rough textures. The Id2 ranges from 98.06% to 100.00%, and Id5 from 97.09% to 100%. These high durability values demonstrate that, despite their very angular shapes, these quartzites possess remarkable resistance to disintegration.

The Pandrang Quartzite samples are very angular (VA), ranging from bladed to equant, featuring rough textures and consistent shapes, with high slake durability indices; Id2 ranges from 98.17% to 100%, and Id5 from 98.17% to 100%. These elevated values indicate that the Pandrang Quartzite samples exhibit excellent resistance to disintegration during wetting and drying cycles.

The Chisapani Quartzite samples display characteristics indicative of a durable rock type and are classified as very angular (VA) with shapes ranging from bladed to equant; the surface texture is consistently rough. The Id2 and Id5 ranges are 98.13% to 100% and 97.20% to 100%, respectively. These high values demonstrate that Chisapani Quartzite is highly resistant to slaking.

Comparing the four types of quartzite samples reveals that their very angular shapes, ranging from bladed to prolate or equant, influence the slake durability indices by increasing the surface area exposed to weathering processes. Nevertheless, the consistently high durability values underscore the role of quartz's inherent hardness, the interlocking grain structure, and rough textures in maintaining structural integrity during slake durability tests. Each quartzite type, despite minor differences in shape and texture, exhibits excellent resistance to disintegration primarily due to these intrinsic properties.

The shape of rock particles significantly influences slake durability values due to their behavior during the slaking process. Distinct shapes affect how rocks disintegrate and influence overall durability assessments (Ersoz, 2024). Irregular or angular particles generally disintegrate more readily compared to rounded ones, impacting durability evaluations. Moon and Beattie (1995) observed that particle shape and size affect slake durability test results, noting that angular particles tend to break down more rapidly during slaking. Similarly, Kolay and Kayabali (2006) found that particle roundness plays a critical role, with more rounded particles demonstrating better durability than angular ones. Particle shape also influences water absorption and weathering; particles with sharp edges or irregular forms have larger surface areas that absorb more water, resulting in increased disintegration during wet-dry cycles. Hopkins and Deen (1984) investigated this phenomenon and found that angular particles degrade faster than rounded ones, which affects slake durability index values. Practically, understanding the influence of particle shape on slake durability is vital for engineering applications such as slope stability and embankment construction. Taylor (1988) emphasized the importance of considering particle shape and texture in evaluating material durability for engineering purposes, as particle shape markedly affects material performance under weathering conditions.

DOI:https//doi.org/10.22452/mjs.vol44no3.4
Malaysian Journal of Science 44(3): 27-49 (September 2025)

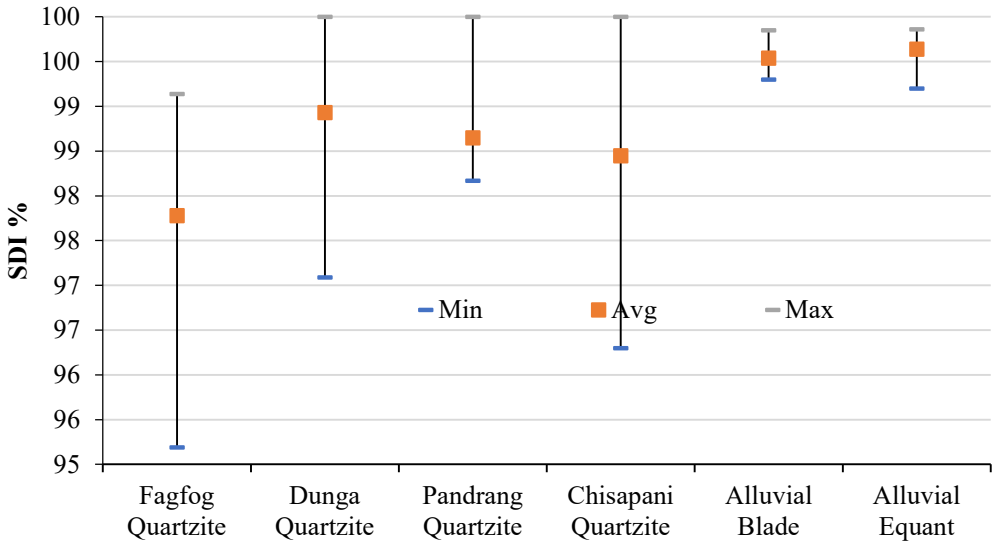

Figure 8. Variation and comparison of SDI among crushed and uncrushed samples

Slake durability index percentages for various quartzite samples—Fagfog Quartzite, Dunga Quartzite, Pandrang Quartzite, and Chisapani Quartzite—together with two alluvial uncrushed samples of blade shape and equant shape, are displayed to clarify their range of variation (Figure 8). Notably, the alluvial uncrushed blade and alluvial uncrushed equant samples exhibit high consistency with minimal differences between their Min, Avg, and Max values, indicating stable and uniform properties. The uncrushed bladed gravel displays an even narrower range (Id2 = 99.68 to 100%, and Id5 = 99.36% to 99.86%) compared to the equant gravel (Id2 = 99.56% to 100%, and Id5 = 99.52% to 100%). Bladed and equant gravels reflect no significant variation in SDI, as they are both subrounded with smooth textures; the loss after the fifth cycle is minimal. Slightly equant samples show more consistent results because their shape reduces stress concentration points, lowering the likelihood of crack propagation during the slake durability tests. Bladed shapes, while still highly durable, have higher length-to-width ratios, making them more susceptible to mechanical breakdown. The increased surface area exposed to weathering processes in bladed shapes can lead to marginally lower resistance to disintegration compared to equant shapes (Figure 8). Conversely, the crushed rock samples display a wide range of SDI variation. The Chisapani Quartzite and the Fagfog Quartzite samples show the broadest range of SDI percentages, suggesting greater variability in their characteristics. Despite this variability, all samples maintain a high average SDI percentage, ranging around 98–99%, reflecting their overall high quality and homogeneity. This analysis highlights the consistency and reliability of the alluvial uncrushed samples compared to the quartzite samples, which exhibit more variation in their SDI percentages.

Effect of Shape on Los Angeles Abrasion Value (LAAV)

The Los Angeles Abrasion Value (LAAV) quantifies the durability of rock aggregates, reflecting their resistance to abrasion and fragmentation. The LAAV varies across different quartzites due to particle shape and other factors. The Fagfog Quartzite shows LAAV values from 12.07% to 31.34%, with lower values indicating better resistance to abrasion despite consistent angularity. The Dunga Quartzite, ranging from 14.89% to 31.32%, also displays variation in LAAV, influenced by factors beyond angularity. The Pandrang Quartzite, with LAAV values from 15.85% to 37.17%, generally exhibits higher abrasion due to its very angular shape. The Chisapani Quartzite has the highest LAAV values, from 22.35% to 48.63%, with extreme angularity and rough texture contributing to severe abrasion. Overall, although high angularity tends to increase LAAV, additional factors such as texture and mineral composition also affect resistance to wear. The angularity of quartzite particles, as noted in the samples, plays a critical role in influencing LAAV values. Very angular particles, with sharp edges and irregular surfaces, typically experience higher abrasion rates compared to more rounded or smooth particles.

For each sample, the minimum, average, and maximum LAAV values are plotted in Figure 9. Notably, the Chisapani Quartzite exhibits the greatest variability in LAAV percentages, with a maximum value around 45%, indicating a broad range of abrasion resistance. In contrast, the Fagfog Quartzite, Dunga Quartzite, and Pandrang Quartzite samples display relatively consistent LAAV percentages, with most values clustering around an average of 25%. Despite variability in maximum values, the average LAAV percentages for all samples from the three formations, except for the Chisapani Quartzite, are similar, suggesting comparable overall abrasion resistance among these quartzite samples.

DOI:https//doi.org/10.22452/mjs.vol44no3.4
Malaysian Journal of Science 44(3): 27-49 (September 2025)

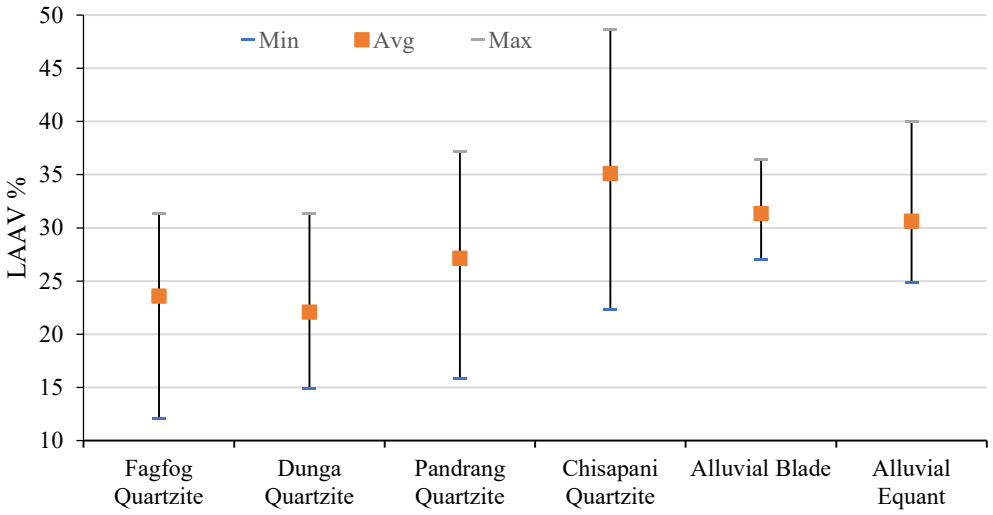

Figure 9. Variation and comparison of LAAV of crushed and uncrushed aggregate samples

When all the crushed and uncrushed samples have been compared for LAAV, the uncrushed samples, though with a narrow range of variation, indicate slightly elevated LAAV, and the average values remain between 30% and 32%, which is marginally higher compared to the values of the Fagfog Quartzite, Dunga Quartzite, and Pandrang Quartzite samples (Figure 9).

The Los Angeles Abrasion Value (LAAV) of uncrushed quartzite samples, characterized by either bladed or equant shapes, exhibits notable variability influenced by particle shape. Bladed shapes generally show higher LAAV values compared to equant shapes (Figure 9). This is because bladed particles, with their elongated and sharp edges, generate more friction and stress during abrasion, leading to greater wear and fragmentation. Conversely, equant-shaped particles, being more compact and less angular, experience reduced friction and stress during abrasion, resulting in lower fragmentation and wear. However, variations within equant and bladed shapes are also observed, influenced by additional factors such as particle size and surface texture. Research by Goswami (1984) and Kazi & Al-Mansour (1980) highlights that highly angular aggregates, such as those with prolate or bladed shapes, tend to have higher LAAV values due to their tendency to interlock and generate more stress during the abrasion process.

Effect of Shape on Sulphate Soundness Value (SSV)

The influence of aggregate shape on SSV is significant. Aggregates with angular shapes tend to have higher SSV values, indicating lower resistance to sulfate weathering. This occurs because the angularity and sharp edges create stress concentration points, making the aggregates more susceptible to fracturing and degradation when exposed to sulfate solutions (Barttli, 1992; Bell, 2007; Koukis et al., 2007).

The Fagfog, Dunga, Pandrang, and Chisapani Quartzite samples collectively illustrate the influence of aggregate shape on Sulphate Soundness Value (SSV) percentages, a measure of resistance to sulfate-induced weathering. All samples are very angular (VA), with shapes ranging from bladed to prolate. The Fagfog Quartzite samples show a wide range of SSV values, 2.91–4.59%, indicating lower resistance to sulfate weathering due to their pronounced angularity and brittleness, which facilitate easier penetration and expansion of sulfate solutions. Similarly, the Dunga Quartzite samples, all very angular and ranging from bladed to prolate, exhibit very low SSV percentages, 0.05–0.48%. In contrast, the Pandrang Quartzite samples demonstrate exceptional resistance to sulfate weathering, with most samples showing 0% SSV despite their very angular nature. This suggests strong internal cohesion and a mineral composition that enhances durability. The Chisapani Quartzite samples also display a low range of SSV percentages, 0–0.74%, with most samples exhibiting 0% SSV, indicating remarkable resistance to sulfate attack. The high resistance in most samples suggests that internal properties, such as mineral composition and geological structure, play crucial roles in durability despite their very angular shape.

DOI:https//doi.org/10.22452/mjs.vol44no3.4
Malaysian Journal of Science 44(3): 27-49 (September 2025)

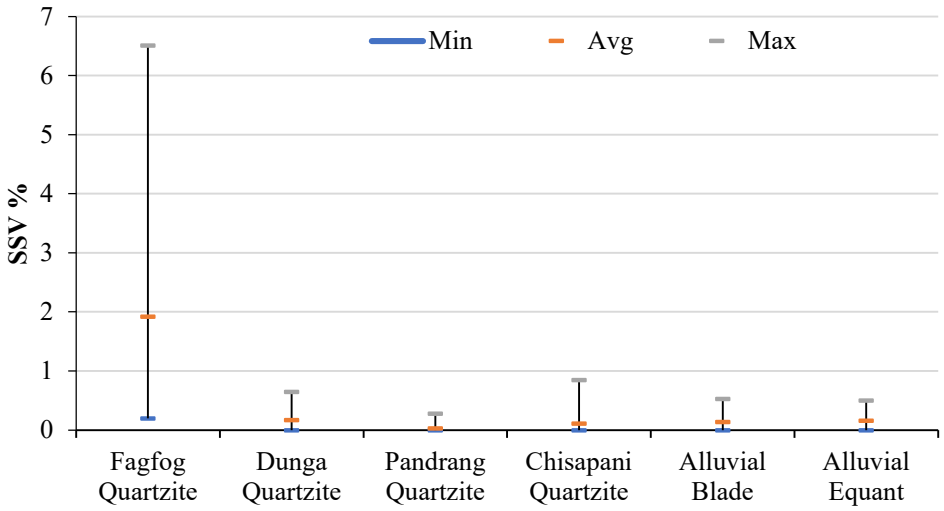

Figure 10. Variation and comparison of SSV of crushed and uncrushed aggregate samples

For each sample, the minimum, average, and maximum SSV values are plotted (Figure 10). Notably, Fagfog Quartzite exhibits a considerable range in SSV percentages, with its maximum value reaching approximately 6.50%, indicating a high degree of shape variability (Figure 10). In contrast, the other samples, including both the remaining quartzite samples and the alluvial samples, display much lower SSV percentages, with maximum values not exceeding 1.50%. This suggests a more uniform shape with less variability. The consistent SSV percentages among the Dunga Quartzite, Pandrang Quartzite, Chisapani Quartzite, blade gravel, and equant gravel indicate similar scattering characteristics and shape uniformity.

The shape of uncrushed quartzite aggregates, specifically bladed and equant, significantly influences the range of Sulfate Soundness Value (SSV) percentages, reflecting their resistance to sulfate-induced weathering. Equant-shaped aggregates tend to exhibit lower SSV percentages, indicating greater resistance to sulfate weathering. Equant shapes generally present a more cohesive structure, which better resists the mechanical stresses induced by sulfate solutions. Conversely, bladed-shaped aggregates tend to demonstrate slightly higher SSV values, reflecting lower resistance to sulfate attack. The increased surface area and edges of bladed particles facilitate easier penetration of the sulfate solution, resulting in higher SSV values.

6. Conclusion

Angular (crushed) quartzite samples show a broader range of PLSI values due to their highly angular shapes and rough textures, which enhance interlocking and mechanical stability. In contrast, uncrushed quartzite samples from alluvial gravel exhibit more consistent and uniformly high PLSI values, owing to their subrounded shapes and smooth textures, which minimize stress concentration points and ensure uniform packing and stress distribution.

Angular (crushed) quartzite samples demonstrate higher resistance to impact and crushing forces due to their pronounced angular shapes, which enhance interlocking and mechanical stability. This leads to higher AIV values but can cause variability in ACV values depending on the extent of voids and stress concentration points. Conversely, uncrushed quartzite samples display more consistent and moderate AIV and ACV values due to their subrounded shapes and smoother textures, which reduce interlocking but ensure uniform stress distribution and packing.

Rounded (uncrushed) samples show greater consistency in slake durability indices due to their smoother and more uniform shapes. In contrast, crushed samples exhibit more variability in SDI values, attributed to their angular shapes and rough textures, which introduce stress concentration points and increase the likelihood of mechanical breakdown.

Angular (crushed) quartzite samples demonstrate better resistance to abrasion, as indicated by their lower LAAV values, attributed to their angular shapes and enhanced interlocking. Conversely, uncrushed quartzite samples exhibit slightly higher LAAV values due to their bladed and equant shapes, with bladed particles showing increased wear and fragmentation during the abrasion process. These findings emphasize the influence of particle shape and texture on the abrasion resistance of quartzite aggregates.

Angular (crushed) quartzite samples, particularly Fagfog Quartzite, show a wider range of SSV values, indicating shape variability that can affect their resistance to sulfate-induced weathering. In contrast, other crushed quartzite samples and alluvial uncrushed samples demonstrate lower and more consistent SSV percentages, indicating uniform shape and enhanced resistance to sulfate attack. Equant-shaped uncrushed aggregates show greater resistance to sulfate weathering compared to bladed-shaped aggregates, which present slightly higher SSV values due to their increased surface area and edges.

DOI:https//doi.org/10.22452/mjs.vol44no3.4
Malaysian Journal of Science 44(3): 27-49 (September 2025)

7. Recommendations

It is recommended that angular (crushed) quartzite be used for load-bearing applications due to its superior interlocking and mechanical stability. For environments requiring consistent strength and durability, uncrushed quartzite with subrounded shapes is preferable. Additionally, the selection of aggregate shapes should be optimized for abrasion resistance and sulfate weathering in specific construction projects. These findings can guide improved material selection in civil engineering, enhancing both performance and durability. Addressing these aspects in future research will enable scientists and engineers to advance the application of quartzite aggregates in civil engineering, leading to improved material performance and sustainability in construction projects.

8. References

Afolagboye, L. O., Talabi, A. O., & Akinola, O. O. (2016). Evaluation of selected basement complex rocks from Ado-Ekiti, SW Nigeria, as source of road construction aggregates. Bulletin of Engineering Geology and the Environment, 75, 853-865.

Ahmad, M., Ansari, M., Sharma, L., Singh, R., & Singh, T. (2017). Correlation between strength and durability indices of rocks-soft computing approach. Procedia Engineering, 191, 458-466.

Aïtcin, P. C. (1998). High performance concrete. CRC Press.

Al-Harthi, A. A. (2001). A field index to determine the strength characteristics of crushed aggregate. Bulletin of Engineering Geology and the Environment, 60, 193-200.

American Concrete Institute. (1991). Standard practice for selecting proportions for normal, heavyweight, and mass concrete (ACI 211.1-91). American Concrete Institute. Retrieved from http://civilwares.free.fr/ACI/MCP04/2211r_98.pdf

American Concrete Institute. (1996). Guide for use of normal weight and heavyweight aggregates in concrete (ACI 221R-96). American Concrete Institute. Retrieved from http://dl.mycivil.ir/dozanani/ACI/ACI%20221R-96%20R01%20Guide%20for%20Use%20of%20Normal%20Weight%20and%20Heavyweight%20Aggregates%20in%20Concrete_MyCivil.ir.pdf

ASTM, A. (2009). C535-09 Standard Test Method for Resistance to Degradation of Large Size Coarse Aggregate by Abrasion and Impact in the Los Angeles Machine. ASTM International, West Conshohocken, PA.

ASTM, D. (2002). 5731. Standard Test Method for Determination of the Point Load Strength Index of Rock and Application to Rock Strength Classifications. ASTM International, West Conshohocken, PA, USA.

ASTM, D. (2008). 4644; Standard Test Method for Slake Durability of Shales and Other Similar Weak Rocks. ASTM International, West Conshohocken, PA, USA.

ASTM. (2005). Standard Test Method for Soundness of Aggregates by Use of Sodium Sulfate or Magnesium Sulfate. ASTM C88-05. ASTM International, West Conshohocken, PA.

Bell, F.G. (2007). Engineering Geology. Butterworth-Heinemann, Oxford, UK, p. 581.

Bista, K., & Tamrakar, N. K. (2015). Evaluation of strength and durability of rocks from Malekhu-Thopal Khola area, Central Nepal Lesser Himalaya for construction aggregates. Bulletin of the Department of Geology, 18, 15-34.

Brattli, B. (1992). The influence of geological factors on the mechanical properties of basic igneous rocks used as road surface aggregates. Engineering Geology, 33(1), 31-44.

British Standards Institution. (1990). Testing aggregates — Part 110: Methods for determination of aggregate crushing value (ACV) (BS 812-110). British Standards Institution.

British Standards Institution. (1990). Testing aggregates — Part 112: Methods for determination of aggregate impact value (AIV) (BS 812-112). British Standards Institution.

BS. (1990). Methods of determination of particle shape. BS 812 105.1, BSI, Flakiness index London. pp. 1–10.

BS. (1990). Testing aggregates Part 105. Methods for determination of particle shape. BS 812 105.2, Elongation index, London, pp. 1-12.

Dhakal, G. P., Kodama, J., & Goto, T. (2006). Freezing-Thawing effect and slake durability of some rocks from cold regions of Nepal and Japan. Journal of Nepal Geological Society, 33, 45-54.

Dhir, R. K., Ramsay, D. M., & Balfour, N. (1971). Study of the aggregate impact and crushing value tests.

Erguler, Z., & Ulusay, R. (2009). Assessment of physical disintegration characteristics of clay-bearing rocks: Disintegration index test and a new durability classification chart. Engineering Geology, 105(1-2), 11-19.

Ersoz, F. (2024). The influence of rock particle shape on slake durability. Journal of Geological Engineering, 12(3), 45-60.

DOI:https//doi.org/10.22452/mjs.vol44no3.4
Malaysian Journal of Science 44(3): 27-49 (September 2025)

Fairhurst, C. E., & Hudson, J. A. (1999). Draft ISRM suggested method for the complete stress-strain curve for intact rock in uniaxial compression. International Journal of Rock Mechanics and Mining Sciences, 36(3), 279-289.

Gautam, P., & Rösler, W. (1999). Depositional chronology and fabric of Siwalik Group sediments in central Nepal from magnetostratigraphy and magnetic anisotropy. Journal of Asian Earth Sciences, 17(5-6), 659-682.

Gautam, T.P., & Shakoor, A. (2013). Slaking behavior of clay-bearing rocks during a one-year exposure to natural climatic conditions. Engineering Geology, 166, 17-25.

Gökceoğlu, C., Ulusay, R., & Sönmez, H. (2000). Factors affecting the durability of selected weak and clay-bearing rocks from Turkey, with particular emphasis on the influence of the number of drying and wetting cycles. Engineering Geology, 57(3-4), 215-237.

Goodman, P.S. (1980). Gamble's slake durability classification. In: Perry, E. (Ed.), Proceedings of the 6th International Congress of the International Association of Engineering Geology, Pergamon Press, Oxford, UK, 331-334.

Goswami, S. C. (1984). Influence des facteurs géologiques sur la qualité et la résistance à l'abrasion des granulats pour couches de surface des chaussées. Bulletin of the International Association of Engineering Geology, 30, 59-61.

Gupta, V., & Sharma, R. (2012). Relationship between textural, petrophysical and mechanical properties of quartzites: a case study from northwestern Himalaya. Engineering Geology, 135, 1-9.

Hachani, M. I., Kriker, A., & Seghiri, M. (2017). Experimental study and comparison between the use of natural and artificial course aggregate in concrete mixture. Energy Procedia, 119, 182–191. doi:10.1016/j.egypro.2017.07.067

Hagen, T. (1969). Report on the geological survey of Nepal, vol. 1. Denkschr. Schwez Naturf. Gesell. Bd., 86(1), 1-185.

Hopkins, T. C., & Deen, R. C. (1984). Identification of shales. Geotechnical Testing Journal, 7(1), 10-18.

Hoskins, J. R., & Horino, F. G. (1968). Effect of end conditions on determining compressive strength of rock samples (Vol. 7171). US Department of the Interior, Bureau of Mines.

International Society for Rock Mechanics. (1981). Rock characterization, testing & monitoring: ISRM suggested methods (E. T. Brown, Ed.). Pergamon Press.

Itihara, M., Shibasaki, T., & Miyamoto, N. (1972). Photogeological survey of the Siwalik Ranges and the Terrai Plain. Southeastern Nepal. Jour. 0/Geosciences, Osaka City Univ, 15(4), 77-98.

Kazi, A., & Al-Mansour, Z. R. (1980). Influence of geological factors on abrasion and soundness characteristics of aggregates. Engineering Geology, 15(3-4), 195-203.

Khanal, S., & Tamrakar, N. K. (2009). Evaluation of quality of crushed limestone and-siltstone for road aggregates. Bulletin of Department of Geology, 12, 20-42.

Kimura, K. (1994). Formation and deformation of river terraces in the Hetauda Dum, Central Nepal a Contribution to the Study of Post Siwalikan Tectonics (Doctoral dissertation, Tohoku University).

Kolay, E., & Kayabali, K. (2006). Investigation of the effect of aggregate shape and surface roughness on the slake durability index using the fractal dimension approach. Engineering Geology, 86(4), 271-284.

Koukis, G., Sabatakakis, N., & Spyropoulos, A. (2007). Resistance variation of low-quality aggregates. Bulletin of Engineering Geology and the Environment, 66, 457-466.

Kuna, E., & Bögöly, G. (2024). Overview of mechanical degradation of aggregates, related standards, and the empirical relations of the parameters. Bulletin of Engineering Geology and the Environment, 83(7), 274.

Lees, G., & Kennedy, C. K. (1975). Quality, shape and degradation of aggregates. Quarterly Journal of Engineering Geology and Hydrogeology, 8(3), 193-209.

Maharjan, S., & Tamrakar, N. (2007). Study of Gravel of the Narayani and Rapti River for Construction Materials. Bulletin of Department of Geology, TU, 10, 99-106.

Mehta, P. K., & Monteiro, P. (2006). Concrete: microstructure, properties, and materials (4th ed.). New York: McGraw-Hill Education.

Moon, V. G., & Beattie, A. G. (1995). Textural and microstructural influences on the durability of Waikato coal measures mudrocks. Quarterly Journal of Engineering Geology and Hydrogeology, 28(3), 303-312.

Neville, A. M. (2011). Properties of Concrete, Pearson Education Limited. Edinburgh Gate, Harlow England, 58-661.

Neville, A. M., & Brooks, J. J. (2015). Concrete technology (2nd ed.). Pearson Education Limited.

DOI:https//doi.org/10.22452/mjs.vol44no3.4
Malaysian Journal of Science 44(3): 27-49 (September 2025)

Podnicks, E. R., Camberlain, P. G., & Thill, R. E. (1968, May). Environmental effects on rock properties. In ARMA US Rock Mechanics/Geomechanics Symposium (pp. ARMA-68). ARMA.

Ramsay, D. M., Dhir, R. K., & Spence, I. M. (1974). The role of rock and clast fabric in the physical performance of crushed-rock aggregate. Engineering Geology, 8(3), 267-285.

Richardson, D. N. (1991). Review of variables that influence measured concrete compressive strength. Journal of Materials in Civil Engineering, 3(2), 95-112.

Schelling, D., Cater, J., Seago, R., & Ojha, T. P. (1991). A balanced cross-section across the Central Nepal Siwalik Hills; Hitauda to Amlekhganj. 北海道大学理学部紀要, 23(1), 1-9.

Smith, M. R., & Collis, L. (2001, January). Aggregates: sand, gravel and crushed rock aggregates for construction purposes. Geological Society of London.

Štambuk Cvitanović, N., Nikolić, M., & Ibrahimbegović, A. (2015). Influence of specimen shape deviations on uniaxial compressive strength of limestone and similar rocks. International Journal of Rock Mechanics and Mining Sciences, 80, 357-372.

Stöcklin, J. (1980). Geology of Nepal and its regional frame: Thirty-third William Smith Lecture. Journal of the Geological Society, 137(1), 1-34.

Stöcklin, J., & Bhattarai, K.D. (1977). Geology of Kathmandu Area and Central Mahabharat Range Nepal. Department of Mines and Geology Kathmandu, Nepal, 86p.

Tamrakar, N. K., Yokota, S., & Shrestha, S. D. (2003). Petrography of the Siwalik sandstones, Amlekhganj-Suparitar area, central Nepal Himalaya. Journal of Nepal Geological Society, 28, 41.

Taylor, R. K. (1988). Coal Measures mudrocks: composition, classification and weathering processes. Quarterly Journal of Engineering Geology and Hydrogeology, 21(1), 85-99.

West, R. M., & Munthe, J. E. N. S. (1981). Cenozoic vertebrate palaeontology and stratigraphy of Nepal. Himalayan Geology, 11, 18-27.

DOI:https//doi.org/10.22452/mjs.vol44no3.4
Malaysian Journal of Science 44(3): 27-49 (September 2025)